Electron–phonon coupling in 122 Fe pnictides analyzed by femtosecond time-resolved photoemission

New Journal of Physics

Electron–phonon coupling in 122 Fe pnictides analyzed by femtosecond time-resolved photoemission

L Rettig[1,2]**, R Cortés**[1,3]**, H S Jeevan**[4]**, P Gegenwart**[4]**, T Wolf**[5]**,
J Fink**[6] **and U Bovensiepen**[2,7]

[1] Fachbereich Physik, Freie Universität Berlin, Arnimallee 14, D-14195 Berlin, Germany
[2] Fakultät für Physik, Universität Duisburg-Essen, Lotharstrasse 1, D-47048 Duisburg, Germany
[3] Abt. Physikalische Chemie, Fritz-Haber-Institut der MPG, Faradayweg 4-6, D-14195 Berlin, Germany
[4] I Physikalisches Institut, Georg-August Universität Göttingen, D-37077 Göttingen, Germany
[5] Karlsruhe Institute of Technology, Institut für Festkörperphysik, D-76021 Karlsruhe, Germany
[6] Leibniz-Institute for Solid State and Materials Research Dresden, PO Box 270116, D-01171 Dresden, Germany
E-mail: uwe.bovensiepen@uni-due.de

Abstract. Based on the results from femtosecond time-resolved photo-emission, we compare three different methods for the determination of the electron–phonon coupling constant λ in Eu- and Ba-based 122 FeAs compounds. We find good agreement between all three methods, which reveal a small $\lambda < 0.2$. This makes simple electron–phonon-mediated superconductivity unlikely in these compounds.

[7] Author to whom any correspondence should be addressed.

IOP Institute of Physics   **Φ** DEUTSCHE PHYSIKALISCHE GESELLSCHAFT

Contents

1. Introduction

Although an enormous amount of research has been conducted in the last few years on the Fe pnictide high-temperature superconductors (HTSCs) [1, 2], the search for the superconducting pairing mechanism in these materials is still ongoing. Besides other excitations such as spin fluctuations [3], the electron–phonon (e–ph) coupling responsible for Cooper pairing in conventional superconductors in the Bardeen–Cooper–Schrieffer (BCS) theory is considered a potential candidate. Therefore the quantitative determination of the e–ph coupling constant λ in the Fe pnictides is of particular interest. Several methods to determine λ have been established in the literature and successfully used in various studies. In the energy domain, angle-resolved photoemission spectroscopy (ARPES) analyzes the renormalization of the single-particle spectral function by the electronic self-energy Σ, which includes the e–ph coupling. However, such type of analysis requires very high sample and data quality, which is difficult to obtain in the Fe pnictides, and only a few ARPES studies of FeAs compounds were able to determine the effects of Σ [4–6]. In addition, in thermal equilibrium, contributions from other degrees of freedom to Σ are often difficult to disentangle from e–ph coupling.

In contrast, femtosecond (fs) time-resolved spectroscopies allow separating of e–ph scattering from other relaxation channels such as e.g. electron–electron (e–e) scattering or heat diffusion due to their different intrinsic timescales out of thermal equilibrium [7–9]. Here, time-resolved ARPES (trARPES) is used, which combines the energy and momentum resolution of ARPES with fs time resolution into a powerful tool to directly investigate the dynamics of the electronic structure in a non-equilibrium state [10, 11].

The e–ph relaxation in metals after photoexcitation has been successfully described using the two-temperature model (2TM) [7–9, 12–14]. This model describes a system of two coupled heat baths for the conduction electrons and the ion lattice with temperatures T_e and T_l by coupled rate equations for T_e and T_l, respectively. One key assumption of this model is that e–e and phonon–phonon (ph–ph) scattering occurs on a much faster timescale than the e–ph scattering, leading to a thermal distribution within each subsystem. However, in correlated electron systems such as the cuprate or Fe pnictide HTSCs, e–ph scattering might occur on similar timescales [15], which poses some questions on the applicability of the 2TM for these materials and care has to be taken. Therefore we analyze our data in terms of a suitable version of the 2TM and compare the results with two complementary methods for the determination of the e–ph coupling strength. We find that all three methods to analyze the e–ph coupling strength
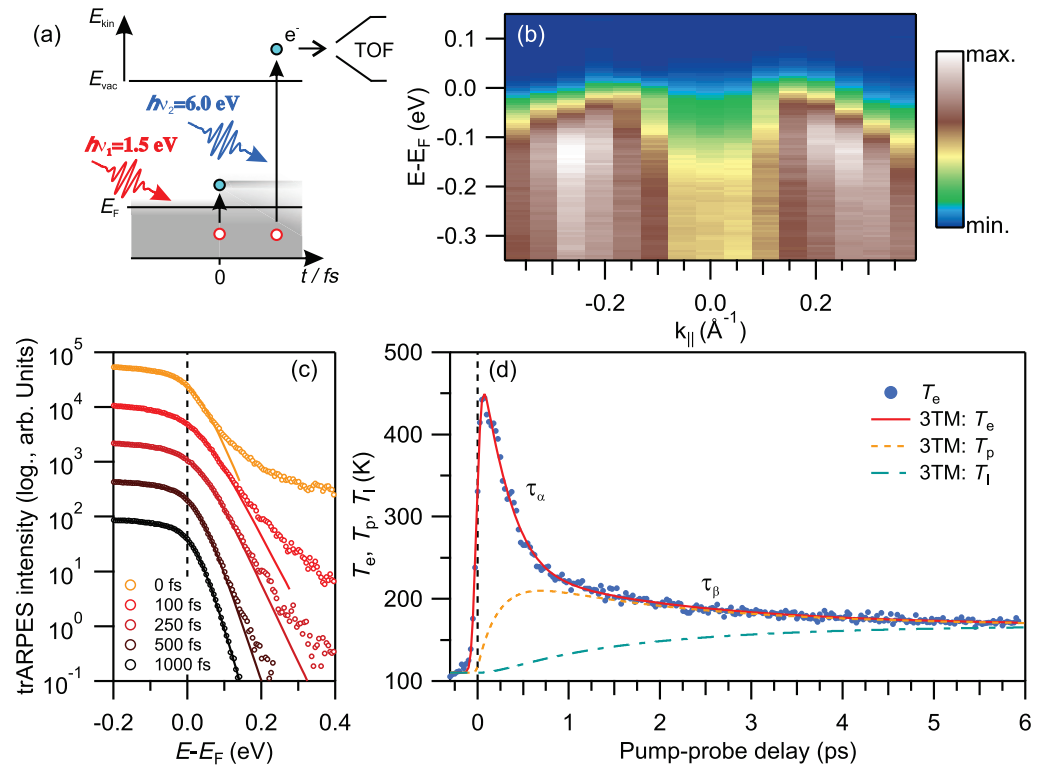
Figure 1. (a) Scheme of the pump–probe experiment. (b) ARPES spectra at $h\nu = 6.0\,\text{eV}$ without excitation in a false color representation, showing the dispersion of the hole pocket in $EuFe_2As_2$. (c) trARPES spectra of $EuFe_2As_2$ at $T = 100\,\text{K}$ and at normal emission for various pump–probe delays on a logarithmic intensity scale using an incident pumping fluence of $F = 0.8\,\text{mJ cm}^{-2}$. Lines are fits to Fermi–Dirac distribution functions. (d) Electronic temperature T_e and a fit to the 3TM. Temperatures of the hot phonons (T_p) and the rest of the lattice modes (T_l) are shown as dashed and dash-dotted lines, respectively.

from time-resolved photoemission data yield results for the second moment of the Eliashberg coupling function $\lambda\langle\omega^2\rangle$, which agree well within error bars and reproduce the trends for three different 122 FeAs compounds consistently.

2. Experiments and results

For trARPES experiments, single crystals of $EuFe_2As_2$ and $BaFe_2As_2$ parent compounds and optimally doped $BaFe_{1.85}Co_{0.15}As_2$ ($T_c = 23\,\text{K}$) were cleaved in ultrahigh vacuum ($p < 10^{-10}$ mbar) at $T = 100\,\text{K}$, where most measurements were carried out. The experimental setup is sketched in figure 1(a): the output of a commercial regenerative Ti:sapphire amplifier (Coherent RegA 9050) delivering ultrashort laser pulses at $h\nu_1 = 1.5\,\text{eV}$ photon energy with a pulse duration of 55 fs, and operating at 300 kHz is used to optically excite the samples (pump pulse). A time-delayed frequency-quadrupled probe pulse at $h\nu_2 = 6.0\,\text{eV}$ photon energy with a pulse duration of 80 fs leads to the emission of photoelectrons, which are detected using an electron time-of-flight (TOF) spectrometer with an acceptance angle of $\pm 3°$. The energy

resolution of 50 meV is mainly determined by the spectral width of the probe pulses, and the overall temporal resolution is < 100 fs. For details see [9].

2.1. Three-temperature model

A dispersion of the hole pocket in $EuFe_2As_2$ without the pump pulse is shown in figure 1(b). Exemplary time-dependent trARPES spectra near Γ are shown in figure 1(c) for various pump–probe delays after excitation on a logarithmic intensity scale. After excitation, a pronounced distribution of excited charge carriers is formed at $E - E_F > 0.1$ eV, which deviates from the Fermi–Dirac distribution of the electronic system before excitation and which originates from hot, non-thermalized electrons. Subsequently, e–e scattering quickly leads to thermalization of these non-thermal electrons and to the formation of a hot thermalized electron distribution [9]. At $t > 250$ fs, the non-thermal contribution has decayed to less than 1% of the electron population.

The temperature of the thermalized part of the electronic system T_e can be extracted from the trARPES data by fitting a Fermi–Dirac distribution function to the high-energy cutoff of the transient spectra, multiplied by a phenomenological density-of-states function and convoluted with an instrumental resolution function [9, 14], as shown in figure 1(c) (solid lines). T_e determined by the fitting is shown in figure 1(d) as a function of pump–probe delay. After the steep rise of the electronic temperature at zero pump–probe delay, we find a relaxation on two distinct timescales τ_α and τ_β. Such a behavior indicates the selective coupling of hot electrons to a subset of strongly coupled phonon modes on the faster timescale τ_α and the subsequent energy transfer to the rest of the phonons by anharmonic ph–ph scattering, determined by τ_β. Thus, the system is described by an extended version of the 2TM, which had been developed for cuprate HTSCs [14], where a similar relaxation dynamics was found, and which has been also used recently for the Fe pnictides [16, 17]. This three-temperature model (3TM) consists of a system of three coupled differential equations describing the temperature of the electrons, T_e, of a hot phonon distribution T_p and of the rest of the lattice modes, T_l:

$$\frac{dT_e}{dt} = -H(T_e, T_p) + \frac{S}{C_e}, \tag{1}$$

$$\frac{dT_p}{dt} = +\frac{C_e}{C_p} H(T_e, T_p) - \frac{T_p - T_l}{\tau_\beta}, \tag{2}$$

$$\frac{dT_l}{dt} = +\frac{C_p}{C_l} \frac{T_p - T_l}{\tau_\beta}. \tag{3}$$

The source term S describes the optical excitation; C_e, C_p and C_l are the specific heat capacities of electrons, strongly and weakly coupled phonon modes, respectively. The anharmonic decay of phonons is described by τ_β. For the energy transfer from the electrons to the more strongly coupled phonons, the formula derived by Allen [7] is used:

$$H(T_e, T_p) = \gamma_T(T_e - T_p) = \frac{3\hbar\lambda\langle\omega^2\rangle}{\pi k_B} \frac{T_e - T_p}{T_e}, \tag{4}$$

where k_B is the Boltzmann constant. This relation allows the determination of the second moment of the Eliashberg e–ph coupling function $\lambda\langle\omega^2\rangle$.

A fit of a numerical solution of the 3TM to T_e is shown in figure 1(d) and yields a good agreement to the experimental data. Owing to an ambiguity of the model parameters such as
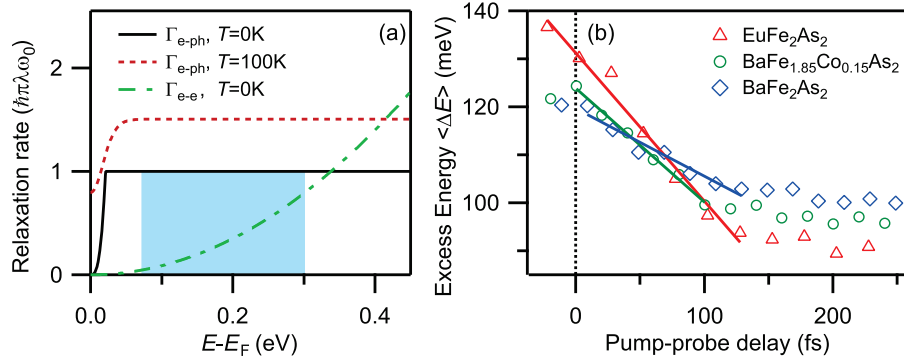
Figure 2. (a) e–ph and e–e contributions to the electron decay rate Γ. The e–ph contribution Γ_{e-ph} calculated in the Debye model with $\hbar\omega_D = 20\,\mathrm{meV}$ and $\lambda = 0.3$ at $T = 0\,\mathrm{K}$ and $T = 100\,\mathrm{K}$ increases up to $\sim \hbar\omega_D$ and is constant above. The electronic contribution Γ_{e-e} calculated for $\beta = 0.1\,\mathrm{eV}^{-1}$ exceeds Γ_{e-ph} only at higher energies. The shaded area marks the energy where e–ph scattering dominates. (b) Electron mean excess energy extracted from trARPES data at $T = 100\,\mathrm{K}$ near k_F within the energy window $0.07\,\mathrm{eV} < \epsilon < 0.3\,\mathrm{eV}$ marked in (a). Solid lines are fits to equation (6).

the electron and lattice specific heat capacities reported in the literature, a range of values for $\lambda\langle\omega^2\rangle$ is retrieved, where the fits show similar good agreement to the data. Details of this analysis can be found in [17]; here, only the main results are discussed. From the 3TM, we find values of $\lambda\langle\omega^2\rangle = 56$–$65\,\mathrm{meV}^2$ for $EuFe_2As_2$, whereas in $BaFe_{1.85}Co_{0.15}As_2$ it is slightly smaller ($\lambda\langle\omega^2\rangle = 46$–$55\,\mathrm{meV}^2$) and even smaller in undoped $BaFe_2As_2$ ($\lambda\langle\omega^2\rangle = 30$–$46\,\mathrm{meV}^2$).

2.2. Electronic excess energy

The analysis within the 3TM was based on the energy relaxation within the thermalized part of the transient electronic distribution function and thus neglected the non-thermal electrons present at early delay times (see figure 1(c)). However, the analysis of the energy relaxation of these non-thermal, excited electrons can also provide information about the strength of e–ph coupling.

The scattering rate of electrons excited at energy $\epsilon = E - E_F$ above the Fermi level is in the self-energy formulation of many-body theory determined by $\Gamma = \hbar\tau^{-1} = 2\mathrm{Im}\,\Sigma(\epsilon)$, where $\mathrm{Im}\,\Sigma$ is the imaginary part of the electronic self-energy [18]. Important energy-dependent contributions to Γ arise from e–e and e–ph scattering, where e–e scattering is considered to follow the quadratic energy scaling of the Fermi liquid theory, $\Gamma_{e-e} = 2\beta[(\pi k_B T)^2 + \epsilon^2]$ (figure 2(a)). As the proportionality coefficient β is rather small in typical metals (of the order of 10^{-2}–$10^{-1}\,\mathrm{eV}^{-1}$) [19, 20], this contribution is negligible compared to the e–ph scattering at low-enough excitation energies. The latter increases up to the maximal phonon energy $\hbar\omega_{max}$ and is constant above (figure 2(a)). For $\epsilon > \hbar\omega_{max}$ and $T = 0\,\mathrm{K}$, Γ_{e-ph} results for an Einstein mode ω_0 to [21]

$$\Gamma_{e-ph} = \pi\hbar\lambda\omega_0. \tag{5}$$

Within the energy window between $\hbar\omega_{max}$ and the crossover regime, where Γ_{e-e} becomes dominant (shaded area in figure 2(a)), the rate of energy dissipation of an electron due to the

emission of a phonon with energy $\hbar\omega_0$ is given by

$$\frac{\mathrm{d}E}{\mathrm{d}t} = \frac{\hbar\omega_0}{\tau} = \pi\hbar\lambda\omega_0^2, \tag{6}$$

which leads to a linear relaxation of the electron energy [22].

The rate of energy relaxation of excited electrons can be extracted from the experimental trARPES intensity $I(\epsilon, t)$ by analyzing the mean excess energy

$$\langle\Delta E(t)\rangle = \frac{\int_{\epsilon_0}^{\epsilon_1} \epsilon\,\Delta I(\epsilon, t)\mathrm{d}\epsilon}{\int_{\epsilon_0}^{\epsilon_1} \Delta I(\epsilon, t)\mathrm{d}\epsilon}. \tag{7}$$

However, this integral represents the mean excess energy within a selected partition of a transient distribution function and not the energy relaxation of single individual electrons. Thus, special care has to be taken with the determination of the integration boundaries, ϵ_0 and ϵ_1. A careful investigation of the influence of the integration boundaries and the excitation fluence reveals that a reasonable choice of $\epsilon_0 = 70\,\mathrm{meV}$ and $\epsilon_1 = 300\,\mathrm{meV}$ allows us to give a good estimate of the e–ph coupling strength, as detailed in [23].

Experimental data of $\mathrm{EuFe_2As_2}$, $\mathrm{BaFe_{1.85}Co_{0.15}As_2}$ and $\mathrm{BaFe_2As_2}$ near k_F and at $T = 100\,\mathrm{K}$ are shown in figure 2(b). To minimize lattice heating and the influence of the hot thermalized electron distribution, low excitation fluences of $F \sim 50\,\mu\mathrm{J\,cm^{-2}}$ have been used. The linear fits to equation (6) within the first 100 fs yield values of $\lambda\langle\omega^2\rangle = 65(5)\,\mathrm{meV^2}$ for $\mathrm{EuFe_2As_2}$, $50(3)\,\mathrm{meV^2}$ for $\mathrm{BaFe_{1.85}Co_{0.15}As_2}$ and $34(6)\,\mathrm{meV^2}$ for $\mathrm{BaFe_2As_2}$. Here, error bars represent the numerical uncertainties of the fits, whereas the overall errors have to be considered larger due to the uncertainty of the integration boundaries discussed above and of the elevated lattice temperature. Nevertheless, we find a good agreement with the values obtained in the 3TM simulations and a considerably higher e–ph coupling in $\mathrm{EuFe_2As_2}$ than in $\mathrm{BaFe_{1.85}Co_{0.15}As_2}$ and even lower $\lambda\langle\omega^2\rangle$ in $\mathrm{BaFe_2As_2}$.

2.3. Temperature-dependent hole relaxation rates

Finally, another estimate of the e–ph coupling strength can be gained from the temperature dependence of quasiparticle (QP) relaxation rates [7, 15, 24, 25]. A recent theoretical investigation of the Boltzmann equation for e–e and e–ph interaction found an analytic solution for the temperature dependence of the QP relaxation rate τ [24]. In the limit of an e–ph scattering rate comparable to or exceeding the rate for e–e scattering and at elevated temperatures, τ depends linearly on the lattice temperature T [15, 24, 25]:

$$\tau = \frac{2\pi k_\mathrm{B} T}{3\hbar\lambda\langle\omega^2\rangle}. \tag{8}$$

This relation allows for an independent determination of the e–ph coupling strength $\lambda\langle\omega^2\rangle$.

Experimentally, the temperature-dependent relaxation of holes in the hole pocket near Γ in $\mathrm{EuFe_2As_2}$ is used, which are found to be independent from the antiferromagnetic transition [26]. The respective hole relaxation time τ_holes is determined from the temperature-dependent trARPES intensity by fitting exponential decay curves (figure 3(a)) and is shown in figure 3(b) as a function of temperature. The fit to equation (8) for $T > 100\,\mathrm{K}$ reveals a good agreement to the linear behavior and yields a value of $\lambda\langle\omega^2\rangle = 90(30)\,\mathrm{meV^2}$, where the error represents a confidence interval of 80%. This value, albeit considerably higher than the values found in the 3TM and in the evaluation of the excess energy, is in agreement with the other evaluations within error bars.
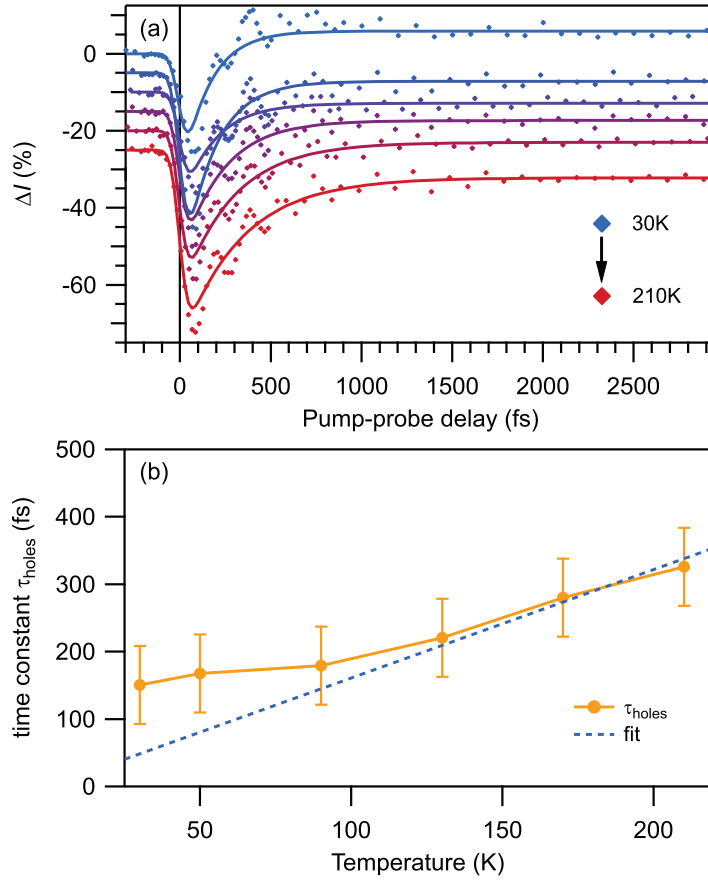
Figure 3. Evaluation of the temperature dependence of relaxation rates in $EuFe_2As_2$. (a) Time-dependent spectral weight of holes at $k_\parallel > k_F$ for various temperatures. Data are vertically offset for clarity. Solid lines are exponential fits (see text). (b) Relaxation time constants τ_{holes} determined from the data in (a) as a function of temperature. The dashed line is a fit to equation (8) in the temperature range $T > 100\,K$.

Table 1. Values of $\lambda\langle\omega^2\rangle$ determined by the three methods.

Compound	$T_e(t)$	$\langle\Delta E(t)\rangle$	$\tau_{holes}(t)$
$EuFe_2As_2$	56–65	65(5)	90(30)
$BaFe_{1.85}Co_{0.15}As_2$	46–55	50(3)	–
$BaFe_2As_2$	30–46	34(6)	–

3. Discussion

The values of $\lambda\langle\omega^2\rangle$ determined by the three methods discussed above are compared in table 1. Despite the limitations and drawbacks of the various methods, we find a perfect agreement of all three methods within error bars. In particular, the trend for larger e–ph coupling in $EuFe_2As_2$ than in $BaFe_{1.85}Co_{0.15}As_2$ and in $BaFe_2As_2$ is well represented.

Remarkably, all methods produce a small $\lambda\langle\omega^2\rangle < 100\,\text{meV}^2$, which already indicates weak e–ph coupling.

Our values of $\lambda\langle\omega^2\rangle$ can be compared to the recently published values determined from optical pump–probe experiments. Mansart *et al* [16] report a comparable value of $\lambda\langle\omega^2\rangle \approx 64\,\text{meV}^2$ for Co-doped BaFe$_2$As$_2$, which was determined using the 3TM. Stojchevska *et al* [25] derived a somewhat higher value of $\lambda\langle\omega^2\rangle = 110(10)\,\text{meV}^2$ in SrFe$_2$As$_2$ using temperature-dependent QP relaxation times, and for SmFeAsO$_{1-x}$F$_x$ an even larger value of $\lambda\langle\omega^2\rangle = 135(10)\,\text{meV}^2$ is reported [27].

Based on our results of $\lambda\langle\omega^2\rangle$ we can estimate the value of the e–ph coupling constant λ for a particular value of ω. Considering the Raman active A$_{1g}$ mode at 23 meV, which can be coherently excited [17, 28, 29] and which therefore shows an enhanced e–ph coupling in the system, we find $\lambda < 0.2$ for all compounds. This estimate is in agreement with the calculations of various Fe-pnictide compounds, which report the values of $\lambda < 0.35$ [30, 31]. Taking the mean of the phonon spectrum as reference, λ gets even smaller, in agreement with other publications [16, 25]. Even if we consider the lowest coupled modes around 12 meV to be most important for e–ph coupling, λ does not exceed a value of 0.5. Similarly small values for λ have been found in the cuprate HTSCs [14, 15], which suggests limited importance of e–ph coupling for the pairing mechanism in both classes of materials.

These boundaries for the e–ph coupling constant λ allow us to estimate the superconducting critical temperature T_c, assuming a conventional BCS-type pairing based on e–ph coupling. Here, T_c in isotropic systems and in a strong-coupling regime is given by McMillan's formula [32], modified by Allen and Dynes [33],

$$T_c = \frac{\omega_{\log}}{1.20} \exp\left(-\frac{1.04(1+\lambda)}{\lambda - \mu^* - 0.62\lambda\mu^*}\right), \tag{9}$$

where μ^* is the effective Coulomb repulsion and $\omega_{\log}$ is the logarithmic average of the phonon spectrum. Taking $\mu^* = 0$ and $\omega_{\log} = 205\,\text{K}$ [30], which provides an upper limit for T_c, we find $T_c = 0.33$ and 7.5 K for $\lambda = 0.2$ and 0.5, respectively. Comparing these results with the experimentally found $T_c = 24\,\text{K}$ in optimally doped BaFe$_{1.85}$Co$_{0.15}$As$_2$ [34] and even up to $T_c = 38\,\text{K}$ in K-doped BaFe$_2$As$_2$ [35] demonstrates that e–ph coupling in a conventional BCS pairing scenario cannot explain the high critical temperatures found in the pnictide HTSCs. In addition, albeit the stronger e–ph coupling, the critical temperatures found in EuFe$_2$As$_2$ upon Co [36] and K [37] substitution are considerably smaller compared to BaFe$_2$As$_2$.

However, e–ph coupling might still play a significant role in the Cooper pair formation in the Fe pnictides. For instance, a very strong sensitivity of the Fe magnetic moment on the As height in the FeAs tetrahedra was found in density functional theory (DFT) band structure calculations [38], with a rate of $6.8\,\mu_B\,\text{Å}^{-1}$. Inelastic x-ray scattering experiments on CaFe$_2$As$_2$ concluded on strong coupling of phonons to magnetic excitations even in the high-temperature paramagnetic phase [39]. Furthermore, a strong sensitivity of the maximum critical temperature on the pnictogen height was found [1]. On the basis of these findings a strong magnetophonon coupling in these compounds was proposed. In particular, the strongly coupled A$_{1g}$ mode perpendicular to the Fe layers, which modulates the pnictogen height, could mediate superconductivity in the Fe-pnictides [40]. Such a scenario is supported by the strong coupling of this particular mode to electronic states directly at the Fermi level [17] evidenced by the coherent excitation of this phonon mode [17, 28, 29].

IOP Institute of Physics   Φ DEUTSCHE PHYSIKALISCHE GESELLSCHAFT

4. Summary

In summary, we demonstrated the quantitative analysis of the e–ph coupling strength from femtosecond trARPES. In detail, we compared three different methods to determine the e–ph coupling strength in three 122 FeAs compounds from time- and angle-resolved photoemission experiments. The transient temperature of the thermalized electronic distribution is analyzed in $EuFe_2As_2$, $BaFe_{1.85}Co_{0.15}As_2$ and $BaFe_2As_2$ by a 3TM; the rate of energy relaxation of the non-thermal electrons yields direct information on the second moment of the Eliashberg coupling function $\lambda\langle\omega^2\rangle$. Finally, the temperature dependence of hole relaxation rates in $EuFe_2As_2$ also allows us to determine $\lambda\langle\omega^2\rangle$. All three methods consistently yield a small $\lambda\langle\omega^2\rangle < 100\,meV^2$, which results in $\lambda < 0.2$ using a reasonable choice of the phonon spectrum. This value is discussed to be too small to explain superconductivity in the Fe pnictides by a conventional BCS-type pairing.

Acknowledgments

References

[1] Johnston D C 2010 The puzzle of high temperature superconductivity in layered iron pnictides and chalcogenides *Adv. Phys.* **59** 803
[2] Stewart G R 2011 Superconductivity in iron compounds *Rev. Mod. Phys.* **83** 1589
[3] Mazin I I, Singh D J, Johannes M D and Du M H 2008 Unconventional superconductivity with a sign reversal in the order parameter of $LaFeAsO_{1-x}F_x$ *Phys. Rev. Lett.* **101** 057003
[4] Wray L *et al* 2008 Momentum dependence of superconducting gap, strong-coupling dispersion kink and tightly bound Cooper pairs in the high-T_c $SrBa_{1-x}(K, Na)_xFe_2As_2$ superconductors *Phys. Rev.* B **78** 184508
[5] Richard P, Sato T, Nakayama K, Souma S, Takahashi T, Xu Y-M, Chen G F, Luo J L, Wang N L and Ding H 2009 Angle-resolved photoemission spectroscopy of the Fe-based $Ba_{0.6}K_{0.4}Fe_2As_2$ high temperature superconductor: evidence for an orbital selective electron-mode coupling *Phys. Rev. Lett.* **102** 047003
[6] Koitzsch A *et al* 2009 Temperature and doping-dependent renormalization effects of the low energy electronic structure of $Ba_{1-x}K_xFe_2As_2$ single crystals *Phys. Rev. Lett.* **102** 167001
[7] Allen P B 1987 Theory of thermal relaxation of electrons in metals *Phys. Rev. Lett.* **59** 1460
[8] Del Fatti N, Voisin C, Achermann M, Tzortzakis S, Christofilos D and Vallée F 2000 Nonequilibrium electron dynamics in noble metals *Phys. Rev.* B **61** 16956
[9] Lisowski M, Loukakos P A, Bovensiepen U, Stähler J, Gahl C and Wolf M 2004 Ultra-fast dynamics of electron thermalization, cooling and transport effects in Ru(001) *Appl. Phys.* A **78** 165
[10] Bovensiepen U, Petek H and Wolf M (ed) 2010 *Dynamics at Solid State Surfaces and Interfaces* vol 1 (Weinheim, Germany: Wiley–VCH)
[11] Bovensiepen U and Kirchmann P S 2012 Elementary relaxation processes investigated by femtosecond photoelectron spectroscopy of two-dimensional materials *Laser Photon. Rev.* **6** 589
[12] Anisimov S I, Kapeliovich B L and Perelman T L 1974 Electron emission from metal surfaces exposed to ultrashort laser pulses *Sov. Phys.—JETP* **39** 375

[13] Rethfeld B, Kaiser A, Vicanek M and Simon G 2002 Ultrafast dynamics of nonequilibrium electrons in metals under femtosecond laser irradiation *Phys. Rev.* B **65** 214303

[14] Perfetti L, Loukakos P A, Lisowski M, Bovensiepen U, Eisaki H and Wolf M 2007 Ultrafast electron relaxation in superconducting $Bi_2Sr_2CaCu_2O_{8+\delta}$ by time-resolved photoelectron spectroscopy *Phys. Rev. Lett.* **99** 197001

[15] Gadermaier C, Alexandrov A S, Kabanov V V, Kusar P, Mertelj T, Yao X, Manzoni C, Brida D, Cerullo G and Mihailovic D 2010 Electron–phonon coupling in high-temperature cuprate superconductors determined from electron relaxation rates *Phys. Rev. Lett.* **105** 257001

[16] Mansart B, Boschetto D, Savoia A, Rullier-Albenque F, Bouquet F, Papalazarou E, Forget A, Colson D, Rousse A and Marsi M 2010 Ultrafast transient response and electron–phonon coupling in the iron-pnictide superconductor $Ba(Fe_{1-x}Co_x)_2As_2$ *Phys. Rev.* B **82** 024513

[17] Avigo I *et al* 2013 Coherent excitations and electron–phonon coupling in $Ba/EuFe_2As_2$ compounds investigated by femtosecond time- and angle-resolved photoemission spectroscopy *J. Phys.: Condens. Matter* **25** 094003

[18] Echenique P M, Pitarke J M, Chulkov E V and Rubio A 2000 Theory of inelastic lifetimes of low-energy electrons in metals *Chem. Phys.* **251** 1

[19] McDougall B A, Balasubramanian T and Jensen E 1995 Phonon contribution to quasiparticle lifetimes in Cu measured by angle-resolved photoemission *Phys. Rev.* B **51** 13891

[20] Valla T, Fedorov A V, Johnson P D and Hulbert S L 1999 Many-body effects in angle-resolved photoemission: quasiparticle energy and lifetime of a Mo(110) surface state *Phys. Rev. Lett.* **83** 2085

[21] Engelsberg S and Schrieffer J R 1963 Coupled electron–phonon system *Phys. Rev.* **131** 993

[22] Gusev V E and Wright O B 1998 Ultrafast nonequilibrium dynamics of electrons in metals *Phys. Rev.* B **57** 2878

[23] Rettig L 2012 Ultrafast dynamics of correlated electrons *PhD Thesis* Freie Universität, Berlin

[24] Kabanov V V and Alexandrov A S 2008 Electron relaxation in metals: theory and exact analytical solutions *Phys. Rev.* B **78** 174514

[25] Stojchevska L, Kusar P, Mertelj T, Kabanov V V, Lin X, Cao G H, Xu Z A and Mihailovic D 2010 Electron–phonon coupling and the charge gap of spin-density wave iron-pnictide materials from quasiparticle relaxation dynamics *Phys. Rev.* B **82** 012505

[26] Rettig L, Cortés R, Thirupathaiah S, Gegenwart P, Jeevan H S, Wolf M, Fink J and Bovensiepen U 2012 Ultrafast momentum-dependent response of electrons in antiferromagnetic $EuFe_2As_2$ driven by optical excitation *Phys. Rev. Lett.* **108** 097002

[27] Mertelj T, Kusar P, Kabanov V V, Stojchevska L, Zhigadlo N D, Katrych S, Bukowski Z, Karpinski J, Weyeneth S and Mihailovic D 2010 Quasiparticle relaxation dynamics in spin-density-wave and superconducting $SmFeAsO_{1-x}F_x$ single crystals *Phys. Rev.* B **81** 224504

[28] Mansart B, Boschetto D, Savoia A, Rullier-Albenque F, Forget A, Colson D, Rousse A and Marsi M 2009 Observation of a coherent optical phonon in the iron pnictide superconductor $Ba(Fe_{1-x}Co_x)_2As_2$ ($x = 0.06$ and 0.08) *Phys. Rev.* B **80** 172504

[29] Kim K W, Pashkin A, Schäfer H, Beyer M, Porer M, Wolf T, Bernhard C, Demsar J, Huber R and Leitenstorfer A 2012 Ultrafast transient generation of spin-density-wave order in the normal state of $BaFe_2As_2$ driven by coherent lattice vibrations *Nature Mater.* **11** 497

[30] Boeri L, Dolgov O V and Golubov A A 2008 Is $LaFeAsO_{1-x}F_x$ an Electron–phonon superconductor? *Phys. Rev. Lett.* **101** 026403

[31] Boeri L, Calandra M, Mazin I I, Dolgov O V and Mauri F 2010 Effects of magnetism and doping on the electron–phonon coupling in $BaFe_2As_2$ *Phys. Rev.* B **82** 020506

[32] McMillan W L 1968 Transition temperature of strong-coupled superconductors *Phys. Rev.* **167** 331

[33] Allen P B and Dynes R C 1975 Transition temperature of strong-coupled superconductors reanalyzed *Phys. Rev.* B **12** 905

[34] Chu J-H, Analytis J G, Kucharczyk C and Fisher I R 2009 Determination of the phase diagram of the electron-doped superconductor $Ba(Fe_{1-x}Co_x)_2As_2$ *Phys. Rev.* B **79** 014506

[35] Rotter M, Tegel M, Johrendt D, Schellenberg I, Hermes W and Pöttgen R 2008 Spin-density-wave anomaly at 140 K in the ternary iron arsenide $BaFe_2As_2$ *Phys. Rev.* B **78** 020503

[36] Jiang S, Xing H, Xuan G, Ren Z, Wang C, Xu Z-A and Cao G 2009 Superconductivity and local-moment magnetism in $Eu(Fe_{0.89}Co_{0.11})_2As_2$ *Phys. Rev.* B **80** 184514

[37] Anupam, Paulose P L, Ramakrishnan S and Hossain Z 2011 Doping dependent evolution of magnetism and superconductivity in $Eu_{1-x}K_xFe_2As_2$ ($x = 0$–1) and temperature dependence of the lower critical field H_{c1} *J. Phys.: Condens. Matter* **23** 455702

[38] Yin Z P, Lebègue S, Han M J, Neal B P, Savrasov S Y and Pickett W E 2008 Electron-hole symmetry and magnetic coupling in antiferromagnetic LaFeAsO *Phys. Rev. Lett.* **101** 047001

[39] Hahn S E *et al* 2009 Influence of magnetism on phonons in $CaFe_2As_2$ as seen via inelastic x-ray scattering *Phys. Rev.* B **79** 220511

[40] Egami T, Fine B V, Parshall D, Subedi A and Singh D J 2010 Spin-lattice coupling and superconductivity in Fe pnictides *Adv. Condens. Matter Phys.* **2010** 164916